Metal-Organic Frameworks with Zero and Low Valent Metal Nodes Connected by Tetratopic Phosphine Ligands

R. Eric Sikma[a] and Seth M. Cohen[a]*

Abstract: *Metal-organic frameworks (MOFs) constructed with M(0) nodes are attractive targets due to the potential reactivity of these low-valent metals, but examples of these MOFs remain exceedingly rare. The rational design of three-dimensional MOFs with Pd(0) and Pt(0) nodes using tetratopic phosphine ligands is reported. Five new MOFs have been synthesized by systematic variation of the phosphine ligands and metal precursors employed, and these represent the first examples of MOFs constructed using phosphine-metal bonds as the only structural component. The MOFs display solid-state luminescence, with emission maxima that are significantly red-shifted compared to $Pd(PPh_3)_4$. In addition, a Rh(I) low valent coordination solid based on the same linker design is reported, which displays solid-state luminescence that is not observed for the molecular analogue.*

Metal-organic frameworks (MOFs) represent a versatile class of porous materials and are of interest for applications including gas storage,[1] separations,[2] and catalysis.[3] MOFs are constructed using multitopic organic linkers, which connect metal ions or metal ion clusters into crystalline, three-dimensional structures.[4] The majority of MOFs are made using anionic organic ligands (e.g., carboxylates) and high oxidation state metal ions (M(II), M(III), M(IV)).[5] This approach limits the scope of organic ligands, metals, and overall materials properties available to MOFs.[6] Notably, the use of hard, anionic ligands precludes the direct incorporation of low-valent metals, which are attractive due to their rich chemistry involving multi-electron processes and catalytic transformations.[7] Numerous strategies have been developed to append low-valent metals to soft Lewis basic sites within MOFs.[8] However, these approaches are limited in scope, result in occupation of free pore volume, and have been less successful for the incorporation of zero-valent metal sites.

Stable complexes of zero-valent metals are well-known, and compounds such as tetrakis(triphenylphosphine)palladium(0) are used widely as pre-catalysts in organic synthesis.[9] These low-valent metal centers require soft Lewis base organic ligands that can act as π-acceptors to form strong, coordinate covalent metal-ligand bonds.[10] Using this guiding principle, Figueroa and co-workers recently reported the first example of a Ni(0) MOF using ditopic organic linkers with isocyanide metal-binding groups.[11] In this case, the low-valent metal was incorporated directly as the metal node of the material, with C-Ni(0) organometallic bonds as the primary structural component. A similar approach has recently been reported for the synthesis of Cr(0), Mo(0), and W(0) materials using pyrazine linkers.[12] Because phosphine ligands are ubiquitous in transition metal chemistry and form strong covalent bonds with soft metals, it was hypothesized that polytopic phosphine ligands could be similarly used to assemble MOFs with low-valent metal nodes.[13]

Lim et al. previously reported several di- and tritopic phosphine ligands, which were found to form metal-organic polyhedra and one-dimensional coordination polymers upon reaction with Cu(I), Ag(I), and Au(I) precursors.[14] These early efforts did not result in structures with higher dimensionality; therefore, tetratopic phosphine ligands with four phosphorus atoms in a tetrahedral orientation were prepared. This arrangement of phosphine donors was expected to discourage the formation of structures with low dimensionality, leading to the assembly of three-dimensional MOF structures. Fortunately, several tetrahedral phosphine ligands were reported by Blümel and co-workers (Figure 1).[15] By varying the central atom and the number of phenyl spacers, a total of four ligands were synthesized using reported methods: **Si1**, **Sn1**, **Si2**, and **Sn2**.

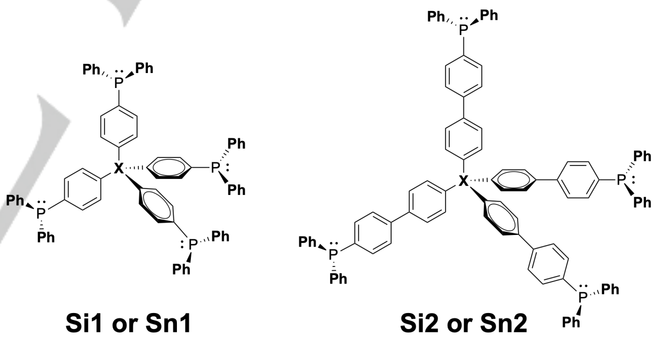

Si1 or Sn1　　**Si2 or Sn2**

X = Si, Sn

Figure 1. Tetratopic phosphine ligands used in this work.

The ligands in Figure 1 were found to rapidly form insoluble, amorphous solids upon exposure to Cu(I) and Ag(I) precursors in a variety of organic solvents. Similar results were obtained by reaction of these ligands with $Pd(PPh_3)_4$, indicating rapid formation of amorphous coordination polymers. Drawing upon existing MOF chemistry, a synthetic strategy was pursued using triphenylphosphine (PPh_3) as a competitive ligand to modulate the coordination of the tetratopic ligands to Pd(0), slowing the formation of coordination polymers.[16]

In the absence of PPh_3, reaction of linker **Si1** with $Pd(PPh_3)_4$ in 1:1 CH_2Cl_2/Toluene (v/v) yielded a poorly crystalline solid (Figure 2). The systematic addition of increasing amounts of PPh_3 to the reaction mixture led to an increase in the sharpness and intensity of diffraction peaks observed by powder X-ray diffraction (PXRD), with 32 equivalents of PPh_3 giving a highly

[a] Dr. R. E. Sikma, Prof. S. M. Cohen
Department of Chemistry and Biochemistry, University of California, San Diego, La Jolla, California 92093, United States.
*scohen@ucsd.edu

Supporting information for this article is given via a link at the end of the document.

crystalline material (Figure 2). Crystals suitable for single-crystal X-ray diffraction (SCXRD) were obtained as yellow tetrahedra using similar conditions in DMF/THF. SCXRD analysis revealed a three-dimensional MOF structure based on the repeat unit Pd(**Si1**) (Figure 3, Figure S1-S3).[17]

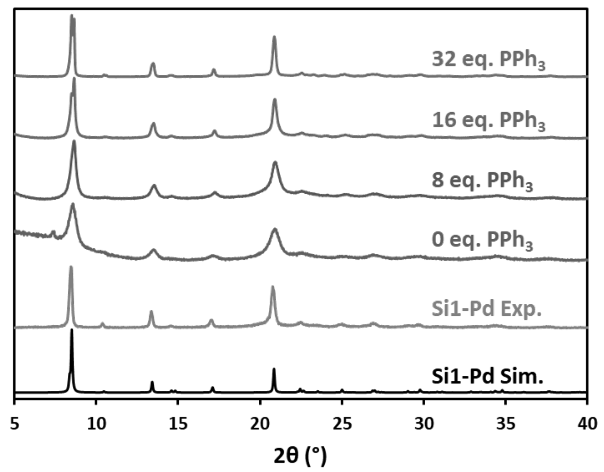

Figure 2. Simulated and experimental PXRD patterns of single-crystalline **Si1-Pd**, with data for bulk samples prepared using varying amounts of PPh_3 modulator.

This new material, **Si1-Pd**, crystallizes in the tetragonal space group *I*−4 and is connected through 4-coordinate Pd(0) nodes, with phosphine donors from four separate **Si1** ligands forming the tetrahedral coordination sphere. The **Si1** linkers are connected to four separate Pd(0) nodes through the phosphine groups, forming a (4,4)-connected diamondoid net (Figure 3, Figure S1-S2). The tetrahedral geometry of the Pd centers indicates that Pd remains in the zero oxidation state in the MOF structure, which is confirmed by the lack of counterions in the SCXRD structure. To the best of our knowledge, this is the first example of a MOF constructed with Pd(0) metal nodes.

Inspection of the three-dimensional structure revealed minimal accessible void space (Figure S3). Accordingly, activated samples of **Si1-Pd** displayed negligible uptake of N_2 in gas sorption experiments (N_2 BET surface area <25 m^2 g^{-1}). When evaluated by thermogravimetric analysis (TGA), **Si1-Pd** remained stable from room temperature to ca. 210 °C, beyond which thermal decomposition occurred (Figure S4). **Si1-Pd** displayed minimal stability in oxygenated solvents, which is typical for molecular complexes of Pd(0). However, under a N_2 atmosphere the MOF displayed excellent stability in a range of polar and nonpolar solvents, including H_2O, as evidenced by retention of crystallinity in the PXRD patterns of **Si1-Pd** exposed to various solvents for 24 h (Figure S5). Dried samples of **Si1-Pd** displayed moderate air stability, with a high degree of crystallinity retained over 24 h in air (Figure S6). Loss of crystallinity was observed over longer time periods, which was accompanied by a distinct color change from bright yellow to orange (Figure S7) and the emergence of a phosphine oxide stretch in the infrared (IR) spectrum (Figure S8), indicating oxidation of the Pd centers and phosphine ligands. However, the MOF was found to be stable indefinitely under inert atmosphere and vacuum.

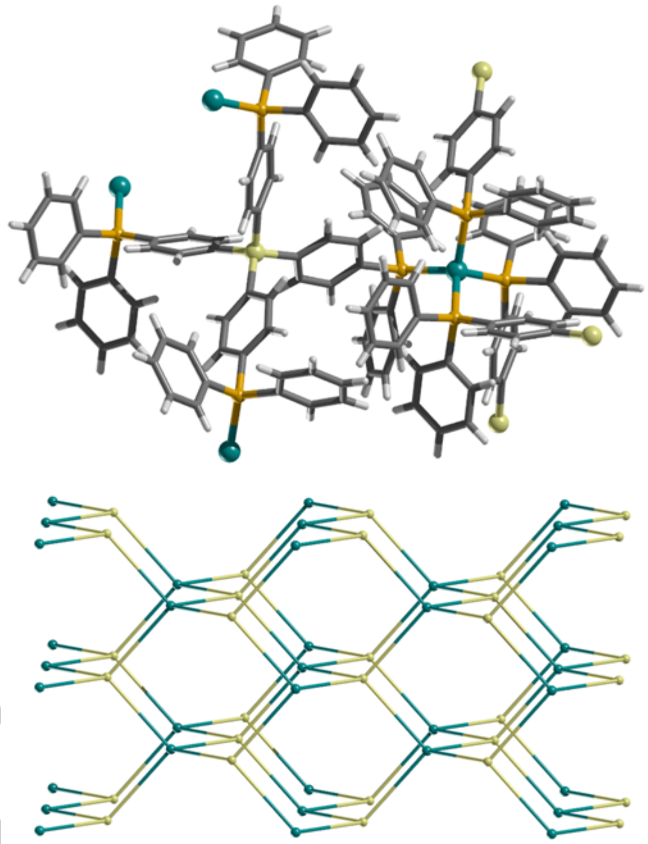

Figure 3. *Top*: View of extended repeat unit in **Si1-Pd** showing full metal and ligand connectivity. *Bottom*: Image of Si−Pd connectivity in **Si1-Pd** showing (4,4)-connected net. Color scheme: C = gray, H = white, P = orange, Pd = teal, Si = yellow.

The modularity of this approach was explored by varying the identity of the main group core atom of the ligand (Si vs. Sn) and the identity of the zero-valent metal (Pd vs. Pt). Reaction of **Sn1** with $Pd(PPh_3)_4$ using 64 equivalents of PPh_3 and otherwise identical reaction conditions gave a highly crystalline material, **Sn1-Pd** (Figure S9). Excellent agreement between the PXRD patterns of **Si1-Pd** and **Sn1-Pd** confirmed the isostructural nature of the materials (Figure 4). The need for significantly more PPh_3 modulator to prepare **Sn2-Pd** suggests differences in the donor properties of **Si1** and **Sn1**, although **Si1-Pd** and **Sn1-Pd** displayed similar thermal and air stabilities (Figure S10-12).

Another isostructural MOF was obtained by reaction of **Si1** with $Pt(PPh_3)_4$, as evidenced by the near-identical PXRD pattern of the resulting material (Figure 4). This represents the first example of a MOF with Pt(0) metal nodes. Notably, **Si1-Pt** displayed enhanced thermal stability compared to **Si1-Pd** and **Sn1-Pd** by TGA, remaining stable to ca. 270 °C, which was attributed to the strength of the P-Pt bonds (Figure S13). The successful synthesis of **Si1-Pt** confirmed that the modularity of the synthesis could be extended to different zero-valent metals.

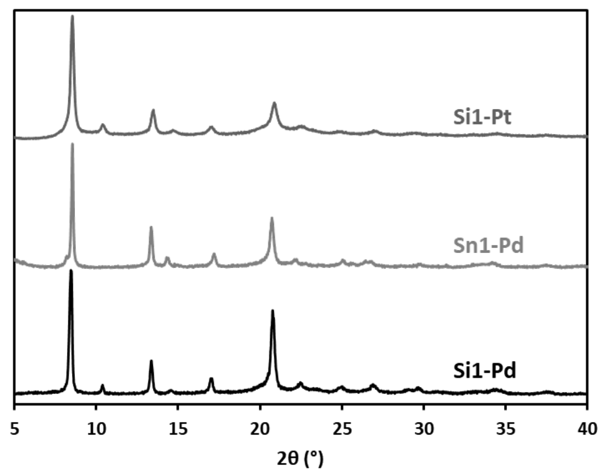

Figure 4. Experimental PXRD patterns of **Si1-Pd** (black), **Sn1-Pd** (red), and **Si1-Pt** (blue).

To further demonstrate the modularity of this approach, MOF synthesis was attempted using the extended **Si2** and **Sn2** ligands (Figure 1). Reaction of **Si2** with $Pd(PPh_3)_4$ and 16 equivalents of PPh_3 yielded single crystals as yellow tetrahedra (Figure S14). When a dried sample of the material was prepared under Ar in a capillary, a PXRD pattern was obtained with several high intensity diffraction peaks at low 2θ values (Figure S15, green trace). This material, **Si2-Pd**, displayed poor air stability, losing bulk crystallinity almost immediately upon exposure to air (Figure S15, blue trace). However, an analogous reaction using **Sn2** and 24 equivalents of PPh_3 yielded quality single crystals with a PXRD pattern matching that of **Si2-Pd** (Figure S15, red trace). SCXRD revealed that an extended MOF had been formed, **Sn2-Pd** (Figure 5, Figure S16-18).[17]

Inspection of the extended structure of **Sn2-Pd** revealed a three-dimensional, interpenetrated network comprised of two independent nets (Figure S16-17), with each net matching the connectivity of **Si1-Pd**. Open channels with a diameter of ca. 7 Å are apparent when viewing the extended structure along the crystallographic b-axis (Figure 5B, Figure S18). The theoretical void volume in **Sn2-Pd** was calculated as 3715 $Å^3$ per unit cell, representing ~20% of the unit cell volume, using a probe radius of 1.82 Å (kinetic diameter of N_2 = 3.64 Å).[18] Imaging this void space revealed accessible open channels weaving through the structure (Figure S19). The same calculation for **Si1-Pd** gave a theoretical void volume of 233 $Å^3$, which is <8% of the unit cell volume, and no open channels were observed (Figure S20). These calculations demonstrate that, despite interpenetration, ligand expansion did have the desired effect of increasing the amount of open space in the MOF structure. However, an activated sample of **Sn2-Pd** was nonporous by N_2 in gas sorption experiments. This was attributed to likely collapse of the pore structure upon activation, as evidenced by loss of crystallinity by PXRD. The dried, but inactivated MOF was found to remain highly crystalline in air for >24 h by PXRD (Figure S21).

Si2-Pd and **Sn2-Pd** are isostructural MOFs in which the only significant difference is the identity of the central atom of the phosphine linker, either Si or Sn. It is therefore remarkable that the two materials display drastically different rates of decomposition in air. The enhanced resistance to oxidation of **Sn2-Pd** suggests a difference in the donor/acceptor properties of **Si2** and **Sn2**.[19] The central atom of the phosphine thus appears to play a significant role in determining the strength of the associated metal−phosphine bonds. Additionally, **Sn2-Pd** was found to remain stable to approximately 270 °C by TGA (Figure S22), which is significantly higher than the decomposition temperature of **Sn1-Pd** (ca. 210 °C, Figure S10). Linker length, which may significantly alter the electronic structure of the ligands, thus appears to be another factor that can influence the stability of these MOFs. These observations demonstrate how linker design can be used to achieve the desired properties (i.e., stability vs. reactivity) in metal−phosphine MOFs.

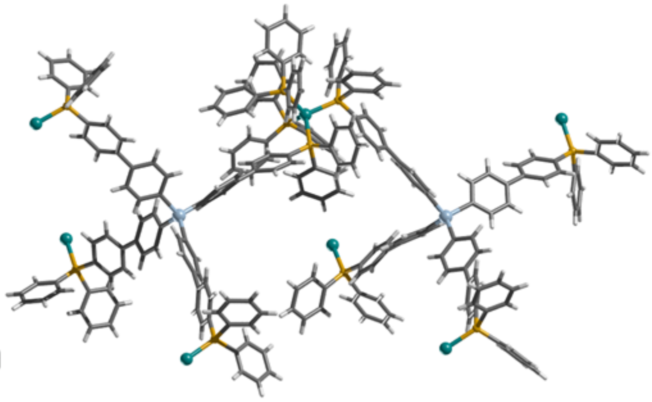

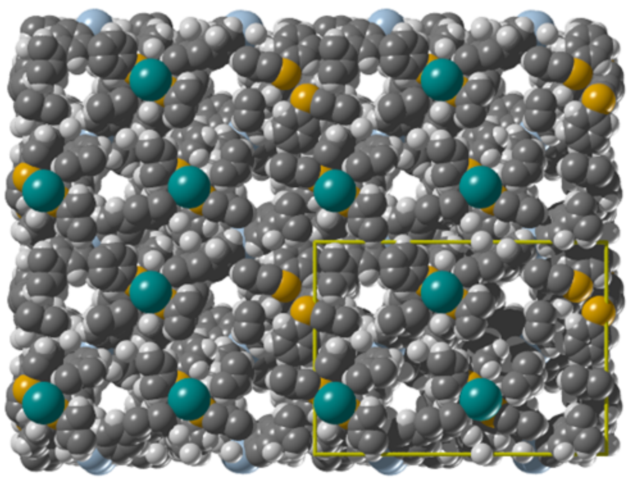

Figure 5. *Top*: View of extended repeat unit in **Sn2-Pd** showing full metal and ligand connectivity. *Bottom*: Space-filling representation of **Sn2-Pd** viewed along the crystallographic b-axis. Color scheme: C = gray, H = white, P = orange, Pd = teal, Sn = blue gray.

In order to further elucidate the structural properties of low-valent MOFs formed from these tetratopic phosphine linkers, materials were targeted containing Rh(I) nodes, which were expected to display lower connectivity through two *trans*-oriented phosphine donors. It was anticipated that formation of diamondoid nets with (2,4)-connectivity, similar to the described Pd(0) and Pt(0) MOFs, would be obtained. Reaction of **Sn1** with $RhCl(CO)(PPh_3)_2$ and 16 equivalents of PPh_3 in THF yielded bright yellow crystals as rounded plates. Interestingly, SCXRD analysis of the material, **Sn1-Rh**, revealed a chain-like structure with one-dimensional connectivity (Figure 6, Figures S23-24).[17] This result demonstrates that free rotation of the phosphine donors allows the linkers to accommodate a variety of geometries, which will thus allow a greater variety of material topologies to be realized. **Sn1-Rh** displayed superior stability relative to the Pd(0) and Pt(0) materials, remaining crystalline after exposure to air for >50 days (Figure S25), after which only a modest increase in the P=O stretch (1184 cm^{-1}) was observed (Figure S26). **Sn1-Rh** displayed excellent thermal stability from room temperature to ca. 340 °C by TGA (Figure S27); this decomposition temperature is ~70 °C higher than the most stable Pd(0) and Pt(0) MOFs. This is also ca. 100 °C than the decomposition temperature of $RhCl(CO)(PPh_3)_2$ (Figure S27), indicating an enhanced Rh−phosphine coordination bond strength relative to Rh−PPh_3.

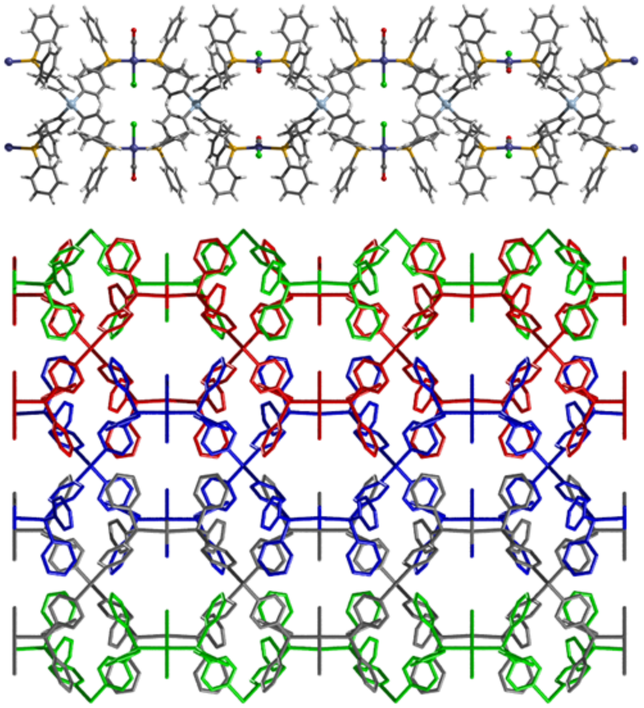

Figure 6. *Top*: image of **Sn1-Rh** crystal structure showing a single one-dimensional chain. Color scheme: C = gray, H = white, O = red, P = orange, Cl = green, Rh = indigo, Sn = blue gray. *Bottom*: Packing of one-dimensional chains in **Sn1-Rh**, with different colors highlighting distinct chains.

The photophysical properties of $Pd(PPh_3)_4$ and several substituted derivatives have been recently investigated.[20] These complexes display strong emission in the solid state, with the emission bands having metal-to-ligand charge transfer (MLCT) character. Emission spectra (λ_{ex} = 360 nm) were collected for dried samples of **Si1-Pd**, **Sn1-Pd**, **Si1-Pt**, and **Sn2-Pd**, which displayed emission maxima at 586, 584, 594, and 667 nm, respectively (Figure S28). These values are significantly red-shifted from the value reported for $Pd(PPh_3)_4$ in the solid state ($\lambda_{em,max}$ = 533 nm). The lower energies of these MLCT bands indicate that **Si1**, **Sn1**, and **Sn2** are stronger π-acceptors relative to PPh_3, which may explain their ability to readily displace PPh_3 as a ligand for Pd(0), even in the presence of excess PPh_3. Although **Sn2-Pd** is only weakly emissive, its observed emission maximum of 667 nm is significantly red-shifted compared to the other materials. This serves as further evidence that linker expansion can have a profound impact on the electronic structures of low-valent MOFs, which in turn dictate their materials properties. Notably, although $RhCl(CO)(PPh_3)_2$ is non-emissive, **Sn1-Rh** was also found to be emissive in the solid-state (λ_{ex} = 330 nm, Figure S28). This emission maximum is significantly blue shifted ($\lambda_{em,max}$ = 524 nm) relative to the Pd(0) and Pt(0) MOFs, while occurring at lower energy than the emission of the free **Sn1** ligand ($\lambda_{em,max}$ = 488 nm, Figure S29).

In summary, this report has described the first examples of MOFs constructed exclusively using metal−phosphine bonds, resulting in the first reported MOF structures with Pd(0) and Pt(0), metal nodes, as well as a unique Rh(I) coordination solid. A modular approach allows these materials to be systematically tuned to achieve enhanced air stability and increased theoretical void space. This opens a new and unexplored class of MOF materials, which will allow for further exploration of solid-state systems incorporating low-valent metals.

Acknowledgements

This work (MOF design, synthesis, and characterization) was supported by a grant from the Department of Energy, Office of Basic Energy Sciences, Division of Materials Science and Engineering under Award No. DE-FG02-08ER46519. Additional support was provided by the Division of Chemistry of the National Science Foundation under Award No. CHE-1661655 for preliminary ligand synthesis studies. The authors acknowledge Dr. Milan Gembicky, Dr. Jake Bailey, and Dr. Mark Kalaj for assistance with X-ray crystallography.

Keywords: metal-organic frameworks • phosphine MOFs • low-valent metals

[1] J. Li, P. M. Bhatt, J. Li, M. Eddaoudi, Y. Liu, *Advanced Materials* **2020**, *32*, 2002563.
[2] R.-B. Lin, S. Xiang, W. Zhou, B. Chen, *Chem* **2020**, *6*, 337-363.
[3] C. Wang, B. An, W. Lin, *ACS Catalysis* **2019**, *9*, 130-146.
[4] C. Gropp, S. Canossa, S. Wuttke, F. Gándara, Q. Li, L. Gagliardi, O. M. Yaghi, *ACS Central Science* **2020**, *6*, 1255-1273.
[5] H. Furukawa, K. E. Cordova, M. O'Keeffe, O. M. Yaghi, *Science* **2013**, *341*, 1230444.
[6] M. Ding, X. Cai, H.-L. Jiang, *Chemical Science* **2019**, *10*, 10209-10230.
[7] R. H. Crabtree, in *Encyclopedia of Catalysis* (Ed.: Horvath), Wiley, New York, **2011**.
[8] a) R. J. Young, M. T. Huxley, E. Pardo, N. R. Champness, C. J. Sumby, C. J. Doonan, *Chemical Science* **2020**, *11*, 4031-4050; b) T. Drake, P. Ji, W. Lin, *Accounts of Chemical Research* **2018**, *51*, 2129-2138; c) S. G. Dunning, G. Nandra, A. D. Conn, W. Chai, R. E. Sikma, J. S. Lee, P. Kunal, J. E. Reynolds Iii, J.-S. Chang, A. Steiner, G. Henkelman, S. M. Humphrey, *Angewandte Chemie International Edition* **2018**, *57*, 9295-9299; d) Y.-S. Wei, M. Zhang, R. Zou, Q. Xu, *Chemical Reviews* **2020**, *120*, 12089-12174; e) J. Zhang, Q. Yang, Y. Zhu, H. Liu, Z. Chi, C.-Y. Su, *Dalton Transactions* **2014**, *43*, 15785-15790.
[9] R. W. Friesen, E. M. D. Allouche, in *Encyclopedia of Reagents for Organic Synthesis*, pp. 1-7.
[10] R. Ugo, *Coordination Chemistry Reviews* **1968**, *3*, 319-344.
[11] D. W. Agnew, I. M. DiMucci, A. Arroyave, M. Gembicky, C. E. Moore, S. N. MacMillan, A. L. Rheingold, K. M. Lancaster, J. S. Figueroa, *Journal of the American Chemical Society* **2017**, *139*, 17257-17260.

[12] L. Voigt, R. Wugt Larsen, M. Kubus, K. S. Pedersen, *Chemical Communications* **2021**, *57*, 3861-3864.
[13] W. Levason, in *Organophosphorus Compounds (1990)*, **1990**, pp. 567-641.
[14] a) S. H. Lim, S. M. Cohen, *Inorganic Chemistry* **2013**, *52*, 7862-7872; b) S. H. Lim, Y. Su, S. M. Cohen, *Angewandte Chemie International Edition* **2012**, *51*, 5106-5109.
[15] a) J. H. Baker, N. Bhuvanesh, J. Blümel, *Journal of Organometallic Chemistry* **2017**, *847*, 193-203; b) Y. Yang, B. Beele, J. Blümel, *Journal of the American Chemical Society* **2008**, *130*, 3771-3773.
[16] R. S. Forgan, *Chemical Science* **2020**, *11*, 4546-4562.
[17] *CCDC Reference Codes: 2091564 (**Si1-Pd**), 2091565 (**Sn2-Pd**), 2121896 (**Sn1-Rh**).*
[18] a) C. F. Macrae, I. Sovago, S. J. Cottrell, P. T. A. Galek, P. McCabe, E. Pidcock, M. Platings, G. P. Shields, J. S. Stevens, M. Towler, P. A. Wood, *Journal of Applied Crystallography* **2020**, *53*, 226-235; b) S. A. Mohamed, J. Kim, *The Journal of Physical Chemistry C* **2021**, *125*, 4509-4518.
[19] M.-K. Hung, K.-W. Tsai, S. Sharma, J. Lei, J.-Y. Wu, S.-A. Chen, *ACS Applied Materials & Interfaces* **2019**, *11*, 36895-36904.
[20] D. Kakizoe, M. Nishikawa, T. Ohkubo, M. Sanga, M. Iwamura, K. Nozaki, T. Tsubomura, *Inorganic Chemistry* **2021**, *60*, 9516-9528.

Entry for the Table of Contents

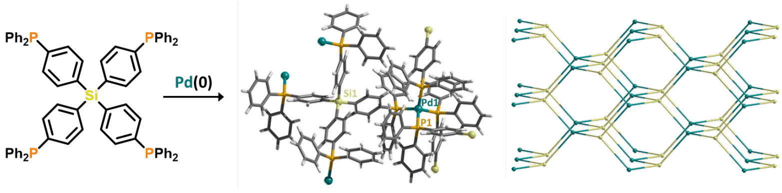

In this work, tetratopic phosphine linkers were used to realize MOFs with Pd(0) and Pt(0) metal nodes, which represent the first MOFs constructed using only metal−phosphine coordination bonds. In addition, a Rh(I) coordination solid was synthesized, highlighting the versatility of these phosphine linkers. A total of six new materials are reported using unique triphenylphosphine-modulated syntheses and their luminescent properties are described.